# Polymer Bulk Erosion

**Achim Göpferich**

*Department of Pharmaceutical Technology, University of Erlangen-Nürnberg, Cauerstrasse 4, 91058 Erlangen, Germany*

*Received November 5, 1996; Revised Manuscript Received February 26, 1997*[⊗]

ABSTRACT: A theoretical model was developed that explains why the erosion of biodegradable bulk-eroding polymers follows the same kinetics on different time scales. poly(D,L-lactic acid-*co*-glycolic acid) 1:1 of various molecular weight served as a model compound. After a period of no mass loss, these polymers erode by spontaneously losing more than half of their mass, which is typical for bulk-eroding polymers in general. Until now this was explained with degradation accelerated by auto catalysis inside the bulk compared to the surface of polymer matrices. To investigate if other mechanisms might be involved as well, an erosion model was developed. It assumes that erosion can start only after the polymers are degraded to water-soluble products and after these degraded polymer areas have contact to the erosion medium. Simulations revealed that percolation phenomena may be responsible for the spontaneous mass loss and that the time of onset is a function of the degradation velocity. Degradation rate constants determined from fits to experimental data of the investigated poly(α-hydroxy esters) agree well with literature values for ester hydrolysis. This suggests that the model is in agreement with existing degradation theories.

## 1. Introduction

For many medical applications the erosion of polymers is a crucial aspect. Erodible polymers control the delivery of drugs to the body, are used in orthopedic surgery as degradable plates and screws that gradually disintegrate during an application,[1] and serve as scaffold material for the repair of tissue and organs.[2] Although these applications depend significantly on the erosion of polymers, little is known about the basic principles according to which erosion proceeds. Until now no universal theory has, for example, been developed to describe the erosion of degradable polymers, nor is there any system that allows to classify these materials according to their erosion behavior. This is surprising because at least some characteristics of erosion have been revealed during the 25 years of research in this area.[3,4] According to what we know, the erosion of water-insoluble degradable polymers starts with degradation, which is the process of chain cleavage. Degradation is followed by the release of degradation products such as oligomers and monomers. This leads to the mass loss of a polymer matrix that is characteristic for erosion.[4] For biodegradable polymers degradation is a chemical process because these polymers are built from functional groups that hydrolyze in an aqueous environment. Hydrolysis starts with the intrusion of water into the polymer bulk. If hydrolysis is slow compared to diffusion, the complete cross section of a polymer matrix is affected by erosion that has been named bulk erosion or homogenous erosion.[5] With increasing degradation velocity, however, erosion becomes a surface phenomenon because water is consumed mainly on the surface by hydrolysis. This has been designated as surface erosion or heterogeneous erosion. Only fast degrading polymers such as polyanhydrides and poly(ortho esters) have been reported to be surface eroding.[6]

A major gap in our knowledge about degradable polymers is the lack of models and theories that describe erosion. Although the erosion of surface-eroding polymers could be described using Monte Carlo models[7] and cellular automata[8,9] it is so far not possible to describe bulk erosion theoretically, which is probably a consequence of the complexity of this process. While the degradation of bulk-eroding polymers usually follows first-order kinetics, their erosion, which is gauged as mass loss, is substantially more complicated. After an initial period of no significant mass loss, erosion usually sets in spontaneously, leading to a rapid mass loss within short periods of time. All bulk-eroding polymers show this erosion behavior, however on different time scales. Low molecular weight poly(D,L-lactic acid) matrices maintain constant mass for a couple of days,[10] high molecular weight poly(D,L-lactic acid) matrices for weeks,[11] and poly(L-lactic acid) or poly(*β*-hydroxybutyrate-*co*-hydroxyvalerate) matrices for months and more.[12,13] It is hard to understand this behavior. One theory explains the sigmoid mass loss profiles of matrices with the autocatalytically accelerated degradation of bulk-eroding polymers. For poly(D,L-lactic acid) and poly(D,L-lactic acid-*co*-glycolic acid) it was for example observed that the acidic degradation products accelerate degradation within polymer matrix disks compared to the surface when eroded in buffer solutions of pH 7.4.[14−16] As a result of this slower degradation on the surface, the outer layers of a matrix exhibit longer mechanical stability. After their erosion to a critical degree, they collapse spontaneously and cause the rapid release of degradation products from within the polymer matrix. This explanation may be valid when pH gradients exist across a polymer matrix cross section, which were indeed found for these polymers during erosion in a pH 7.4 buffer. While the pH on the surface was maintained by the buffer, inside these polymers values as low as pH 2 were measured.[17,18] However, when the same polymers were eroded at pH 2 to enforce that no pH gradients exist, the same discontinuous mass loss profiles were obtained. This shows that autocatalytic effects alone cannot account for the results. The intention of this study was to find additional mechanisms that might be responsible for the discontinuous mass loss of bulk-eroding polymers. The theoretical approach described here is intended to give deeper insight into the complicated erosion process of bulk-eroding polymers and to facilitate the application of this class of biomaterials in the future.

[⊗] Abstract published in *Advance ACS Abstracts,* April 1, 1997.

S0024-9297(96)01627-0 CCC: $14.00 

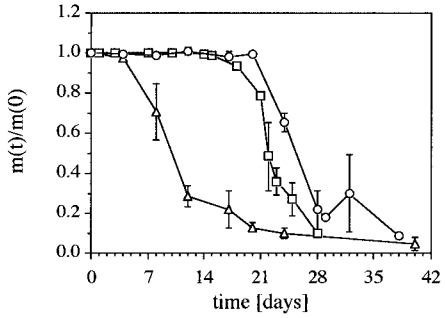


**Figure 1.** Mass loss during the erosion of polymer matrix disks: (△) RG 502H; (□) RG 504H; (○) RG 502.

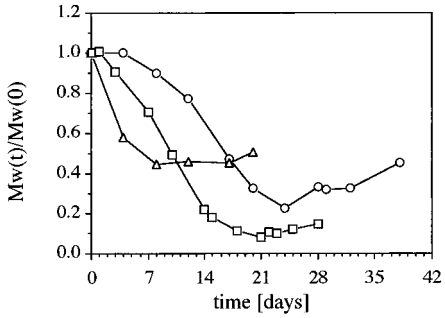


**Figure 2.** Loss of molecular weight due to polymer degradation: (△) RG 502H; (□) RG 504H; (○) RG 502.

## 2. Materials and Methods

**2.1. Materials.** Poly(D,L-lactic acid-*co*-glycolic acid) with molecular weight 8000 (Resomer RG 502H), 14000 (Resomer RG 502) and 47000 (Resomer RG 504H) were obtained from Boehringer Ingelheim, Ingelheim, Germany. Polystyrene standards with a narrow molecular weight distribution were purchased from Phenomenex, Torrance, CA. Chloroform was purchased from Fluka, Buchs, Switzerland.

**2.2. Methods. The Erosion of Polymer Matrix Disks.** Cylindrical polymer matrix disks with a diameter of 8 mm and a height of approximately 1 mm were prepared by melt casting using Teflon molds.[19] The polymers were melted at 120 °C inside the molds and slowly cooled to room temperature under ambient conditions. The samples were eroded in 10 mL of 0.1 M phosphate buffer, pH 7.4, which was changed regularly. Prior to the determination of mass loss, solid samples were vacuum dried for approximately 24 h using a RV5 vacuum pump from Edwards High Vacuum International, Crawley, Sussex, England, until a final pressure of 0.5 Pa was reached.

**Determination of Molecular Weight.** Molecular weights were determined using gel permeation chromatography. Separations were performed using an LC 250 Pump and an ISS200 autosampler from Perkin-Elmer, Newton Center, MA. As stationary phase, a 5 $\mu$m 300 × 7.8 mm mixed bed Phenogel column (MW range 0−10 000K) in combination with a 5 $\mu$m 300 × 7.8 Phenogel column with a pore size of 500 Å (MW range 500−10K) and a guard column, all from Phenomenex, Torrance, CA, were used. Chloroform served as mobile phase with a flow rate of 1 mL/min. Spectra were recorded using an ERC-7515A refractive index detector from Erma CR. Inc., Tokyo, Japan. The cell temperature was maintained at 30 °C. The signal was digitized using a Nelson 950 interface from Perkin-Elmer, Newton Center, MA. Typical retention times were between 12 and 21 min. The columns were calibrated using 10 different polystyrene standards with narrow molecular weight distribution ranging from 208 to 79 000 kD. Molecular weights were calculated from the chromatograms of samples using TC-SEC size exclusion chromatography software from Perkin-Elmer, Newton Center, MA.

**Calculations and Simulations.** All calculations and simulations were performed on Macintosh computers. The software was written in Pascal using a Think Pascal compiler from Symantec, Cupertino, CA.

## 3. Results and Discussion

**3.1. Mass Loss (Erosion).** The erosion of poly(D,L-lactic acid-*co*-glycolic acid) matrix disks leads to mass loss profiles that are typical for bulk-eroding polymers (Figure 1). The mass loss profiles have the same shape for all investigated polymers and consist of two parts. During the first period there is no significant loss of mass. During the second period the mass loss sets in spontaneously. The time at which erosion starts depends on the molecular weight of the polymer and the state of the COOH terminal. End-capped polymers in which the −COOH terminal is linked to an alcohol via an ester bond to control the molecular weight during synthesis such as RG 502 characteristically exhibit longer stability compared to the corresponding polymers with free carboxylic acid end groups such as RG 502H and RG 504H. The erosion characteristics are not only typical for cylindrical matrix disks but were also found for other geometries made of these polymers such as thin films,[20] long cylinders,[17] and even microspheres.[21] It is not obvious why the mass of the matrices remains unchanged for a long period of time prior to its rapid decline.

**3.2. Molecular Weight Loss (Degradation).** To investigate the cause of constant mass during early times of erosion, molecular weight changes were determined by GPC. The molecular weight serves as a measure for polymer degradation, which is a necessary condition for the erosion of these polymers as all three polymers have to degrade substantially before water-soluble degradation products are formed. Figure 2 shows the relative change of molecular weight during the erosion of the investigated bulk-eroding polymers. In all cases, the molecular weight loss follows a sigmoid profile. After an initial lag period, the degradation rates increase. In general one can see that the degradation velocity depends on the molecular weight of the polymers. The lower the molecular weight, the faster the degradation. Equally important is the use of molecular weight controlling substances that might be incorporated into the polymer backbone during synthesis. End-capped RG 502 degrades substantially slower compared to RG 502H and RG 504H. Most important with respect to the interpretations of the shape of the erosion profiles is the fact that degradation starts immediately after the start of the erosion experiment. Therefore, the initially constant mass cannot be explained with the lack of degradation early during the experiment.

**3.3. The Development of an Erosion Model.** An explanation for the constant mass during early times of erosion would be that the polymers have to reach a critical molecular weight below which they are water soluble and can be released from the matrices. That this mechanism has certainly an impact on erosion can be seen from the dependence of erosion on the molecular weight. Figures 1 and 2 show that the erosion of the investigated poly(D,L-lactides-*co*-glycolides) depends strongly on molecular weight. The hypothesis of degradation to a critical molecular weight, however, cannot explain the constant mass of these polymers early during erosion. Assuming that degradation is a random process which may affect each bond in the polymer backbone with equal probability, low molecular weight compounds are created right from the beginning of the erosion. If they can be released immediately, they should cause a mass loss right from the beginning of the erosion experiment, which is obviously not the case.

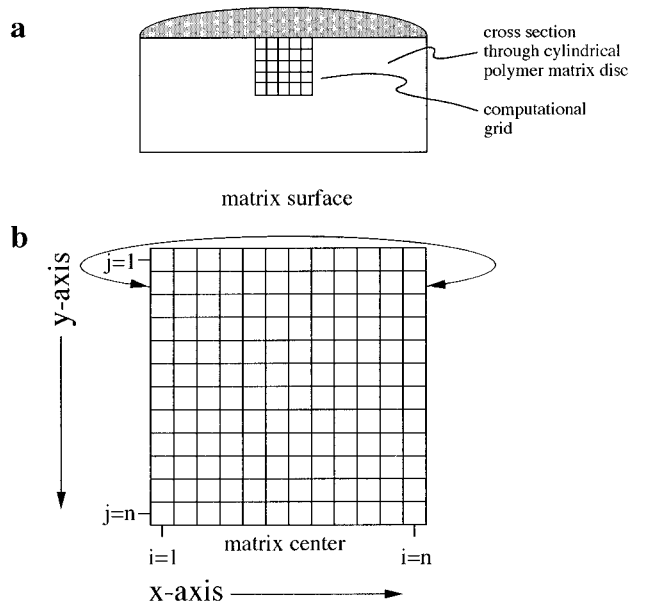


**Figure 3.** Schematic representation of a polymer matrix cross section by a rectangular grid: (a) location of the grid on the cross section of a cylindric matrix disk; (b) computational grid in detail.

The goal of the modeling approach is to describe polymer bulk-erosion theoretically and to explain why erosion does initially not affect the mass of bulk-eroding polymer matrix disks despite the degradation of the polymer. To keep the model as simple as possible, swelling is not taken into account. The experimental investigations showed that the mass loss lags behind the loss of molecular weight. Therefore it is necessary to distinguish between polymer degradation, which is reflected by the molecular weight loss, and erosion, which is characterized by the mass loss. It is assumed that degradation is a necessary condition for the erosion of water insoluble polymers and that degraded polymer can only erode after it has contact to a pore or the matrix surface. Three major steps are involved in developing a model that accounts for these phenomena:

1. Polymer cross sections have to be represented theoretically by a two-dimensional rectangular grid that divides the matrix into a multitude of small polymer pieces (pixels).

2. Each pixel has to be assigned an individual lifetime. The pixels are then "degraded" in the sequence of their lifetime and considered eroded after they come into contact with a pore.

3. From the time-dependent "disappearance" of pixels, functions for erosion and degradation have to be defined that correspond to the experimentally determined functions. These functions are intended to allow one to compare the model with experimental data.

**3.3.1. The Representation of Polymer Matrix Disks.** Polymer matrix disks are represented in two dimensions by covering a part of the cross section with a rectangular grid as shown schematically in Figure 3a. Figure 3b shows the grid in more detail. The grid has $n \times n$ grid points. The $x$-axis is parallel to the cylinder surface, and the $y$-axis is perpendicular to it. The grid line $j = 1$ represents the cylinder surface; the grid line $j = n$, the center of the matrix. To reduce the amount of calculations only half of the cross section is covered in the vertical direction, because the erosion problem is symmetric with respect to the cylinder axes. The grid is also truncated in horizontal direction along the lines $i = 1$ and $i = n$. To avoid errors due to this reduction, periodic boundary conditions are applied to these grid sites. This connects the pixels at both ends of the grid as indicated schematically in Figure 3b. The individual pixels $P_{i,j}$ are assigned one of the following three properties: nondegraded, degraded, or eroded. The variable $x_{i,j}$ defines these states:

$$\begin{aligned} x_{i,j} &= 1 \quad \text{nondegraded} \\ x_{i,j} &= 0 \quad \text{degraded} \\ x_{i,j} &= -1 \quad \text{eroded} \end{aligned} \tag{1}$$

As a starting condition one assumes that $x_{i,j} = 1$ at $t = 0$ for all $P_{i,j}$ ($1 \le j \le n$, $1 \le i \le n$) because all pixels on the grid represent initially nondegraded polymer. The boundary conditions require the introduction of four hypothetical grid lines for computational reasons: $P_{i,0}$ and $P_{i,n+1}$ ($1 \le i \le n$) as well as $P_{0,j}$ and $P_{n+1,j}$ ($1 \le j \le n$). On these grid lines the variable $x_{i,j}$ is defined as follows:

$$\left.\begin{aligned} x_{i,0} &= -1 \\ x_{i,n+1} &= x_{i,n-1} \\ x_{0,j} &= x_{n,j} \\ x_{n+1,j} &= x_{1,j} \end{aligned}\right| \; 1 \le i \le n;\ 1 \le j \le n \tag{2}$$

**3.3.2. Simulation of Degradation and Erosion.** To simulate degradation, first the lifetime of pixels has to be determined. Once this lifetime, expires the pixel is considered degraded and its status is changed from $x_{i,j} = 1$ to $x_{i,j} = 0$. The calculation of polymer lifetimes until degradation is based on the assumption that the degradation of individual pixels is a Poisson process. The lifetimes are then distributed according to a first-order Erlang probability density function:[22]

$$e(t) = \lambda e^{-\lambda t} \tag{3}$$

$e(t)$ is the probability that a pixel degrades at time $t$, $\lambda$ is a degradation rate constant, and $t$ is the random variable that designates the lifetime, that is the time between the start of the experiment and the "degradation" of a pixel. When using eq 3 one has to consider the dependence of $e(t)$ on the grid size $n$. For large $n$, a grid needs a longer time until complete erosion compared to a grid with small $n$. To overcome this problem, eq 3 was corrected for the grid size. This was achieved by considering the expected value of $t$, which is obtained from eq 3 by integration with respect to $t$ in the interval $[0,\infty]$. This yields

$$e(t)_{\exp} = \frac{1}{\lambda} \tag{4}$$

$e(t)_{\exp}$ is the expected lifetime of a pixel. The grid consists, however, of a multitude of pixels. Therefore, the expected time until all pixels are "degraded" has to be considered. When the "degradation" of an individual pixel follows Poisson kinetics, the degradation of all pixels does also follow Poisson kinetics.[22] The expected value in that case can be calculated from eq 5. $e(t)_{\exp_n}$

$$e(t)_{\exp_n} = \frac{1}{\lambda} + \frac{1}{2\lambda} + \frac{1}{3\lambda} + \ldots + \frac{1}{n^2\lambda} \tag{5}$$

is the expected lifetime for the disappearance of all pixels from a grid of size $n \times n$. Equation 5 can be

rearranged to obtain

$$e(t)_{\exp_n} = \frac{1}{\lambda} \sum_{i=1}^{i=n^2} \frac{1}{i} \tag{6}$$

The sum in eq 6 can be approximated as $\ln(n^2)$ which yields

$$e(t)_{\exp_n} = \frac{1}{\lambda} \ln(n^2) \tag{7}$$

If $\lambda$ in eq 3 is replaced by $\lambda \ln(n^2)$, eq 8 is obtained,

$$e(t)_n = \lambda \ln(n^2)\, e^{-t\lambda[\ln(n^2)]} \tag{8}$$

for which the values of expectation are independent of the grid size for sufficiently large $n$. To simulate degradation, the lifetimes of pixels have to be calculated from eq 8 at random. This is achieved by using Monte Carlo sampling techniques.[23] In brief: first, eq 8 is integrated with respect to $t$ in the interval $[0,\infty]$ which yields the probability that a pixel erodes within this time interval. The resulting equation is set equal to $\epsilon$, a random variable equally distributed in the interval [0,1], which yields

$$t_{i,j} = \frac{1}{\lambda \ln(n^2)} \ln(1 - \epsilon) \tag{9}$$

$t_{i,j}$ is the time at which a pixel $P_{i,j}$ degrades. Values of $t_{i,j}$ are calculated at random from eq 9 by generating random numbers $\epsilon$ on the computer and substituting them into eq 9.

To simulate erosion, the lifetime of all $n^2$ pixels are calculated prior to the start of a simulation. The pixels are then degraded in the sequence of their lifetimes. Once the lifetime of a pixel $P_{i,j}$ expires, it is assumed to be degraded. Degradation of a pixel, however, cannot lead to the erosion of the grid site as long the mass loss is prevented by nondegraded neighbors. Only if at least one of the eight neighboring pixels is already eroded can a degraded pixel release its degradation products into the erosion medium and be finally regarded as eroded. This is taken into account with the model by updating the values $x_{i,j}$ of the complete grid according to eq 10 after the degradation or erosion of any grid site.

$$x_{i,j} = \begin{cases} 0 & | x_{k,l} \neq -1;\ i-1 \le k \le i+1;\ j-1 \le l \le j+1 \\ -1 & | x_{k,l} = -1;\ j-1 \le k \le j+1;\ j-1 \le l \le j+1 \\ 1 & | \text{else} \end{cases} \tag{10}$$

The changes that a grid undergoes during erosion are illustrated in Figure 4, which shows a model simulation. The pattern of the pixels in the figure reflect the status of a pixel. Nondegraded polymer is shown in black, degraded polymer in gray, and eroded polymer in white. Early during the erosion ($\lambda t = 0.08$), the degraded pixels are distributed all over the grid and are insulated from one another. Only pixels on the surface, i.e. in the top row of each figure at $j = 1$, have access to the erosion medium and can, therefore, erode at this early time. At $\lambda t = 0.047$, the degraded pixels are increasingly connected to one another and start to form clusters. When one member of such a cluster erodes, the complete cluster erodes spontaneously at the same time because the erosion condition is fulfilled for all pixels that belong to it. This phenomenon can be observed between $\lambda t = 0.047$ and $\lambda t = 0.06$ when large parts of the grid erode in a short period of time. From these simulations a very important conclusion can be drawn: under the assumptions that were made, percolation phenomena become involved in polymer erosion. Erosion can start only after the degraded pores belong to a percolation cluster that connects them to the "surface". This happens after the matrix has degraded to a critical degree, and large parts of the grid erode spontaneously after the degradation of only a few pixels.

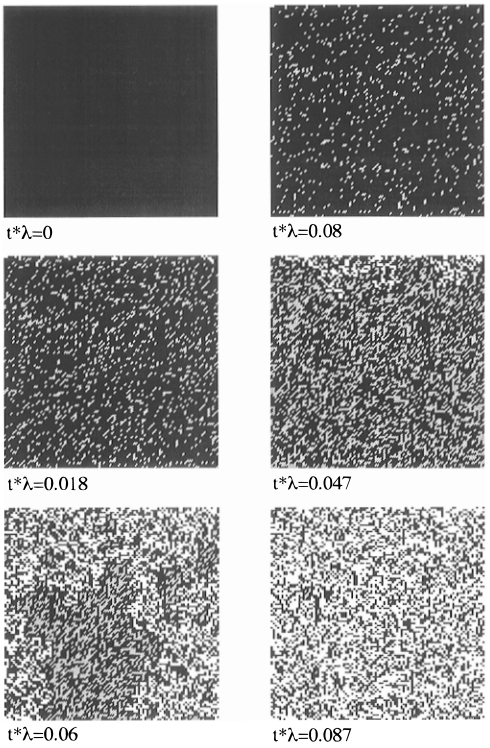


**Figure 4.** Simulation of erosion: (black) nondegraded polymer; (gray) degraded polymer; (white) eroded polymer (pores).

**3.3.3. The Evaluation of Simulations.** To be able to compare the model simulations with experimental data, functions have to be found that correspond to the experimental data of degradation and erosion. The degree of polymer degradation can be followed, by determining the relative number of nondegraded pixels:

$$d(t) = \frac{1}{n^2} \sum_{i=1}^{i=n} \sum_{j=1}^{j=n} s(x_{i,j}); \qquad s(x_{i,j}) = \begin{cases} 1; & x_{i,j} = 1 \\ 0; & \text{else} \end{cases} \tag{11}$$

Erosion can be gauged in terms of mass loss. Equation 12 calculates the relative mass from erosion simulations.

$$m(t) = \frac{1}{n^2} \sum_{i=1}^{i=n} \sum_{j=1}^{j=n} s(x_{i,j}); \qquad s(x_{i,j}) = \begin{cases} 0; & x_{i,j} = -1 \\ 1; & \text{else} \end{cases} \tag{12}$$

The functions defined by eqs 11 and 12 were calculated from simulations and are shown in Figure 5 in nondimensional form. The curve representing degradation drops right from the start of the simulation. This is characteristic for the algorithm, because the likelihood to degrade drops exponentially with increasing time. The erosion curve behaves differently. Prior to the existence of percolation clusters there is almost no mass loss and therefore no erosion. The spontaneous mass loss sets in after approximately 50% of the pixels are degraded which is at $t\lambda = 0.05$. The erosion curve

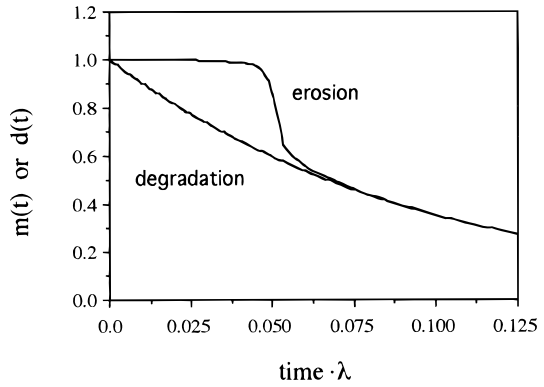


**Figure 5.** Erosion and degradation curve obtained from a simulation using a gridsize $n = 175$ (average of five simulations).

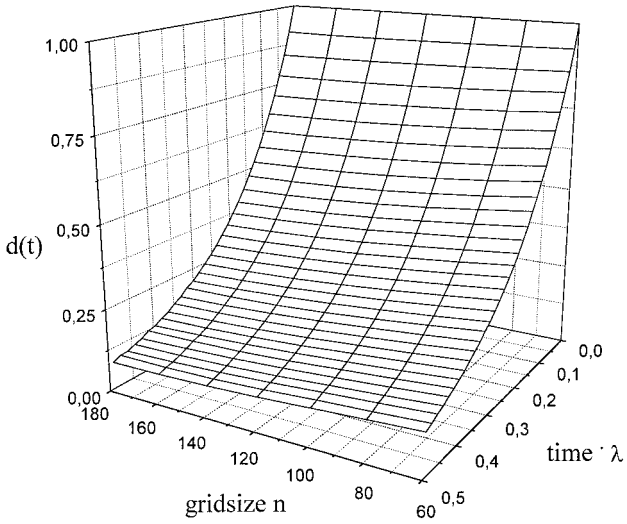


**Figure 6.** Degradation curves as a function of the gridsize $n$ (average of five simulations).

follows the degradation curve after this sudden drop because all further pixels that degrade are most likely connected to a percolation cluster and, therefore, are considered eroded at the time they degrade.

**3.3.4. The Determination of the Optimal Grid Size.** For sufficiently large $n$ the results that are obtained from the simulations above are independent of the grid size. Large grids increase, however, the amount of calculations substantially. Small grids, on the other hand, allow fast simulations but may yield inaccurate and instable results. Therefore, prior to working with the model the grid size has to be determined that is at least needed to obtain accurate and stable results. For that purpose, the degradation and erosion profiles were determined as a function of the grid size $n$. In Figure 6 the theoretical degradation profiles are shown as a function of time and grid size. For grids larger than $n = 150$, the results are identical. The same was observed for the erosion profiles, which are shown in Figure 7. There are only minor changes in the curve profiles when increasing the grid size above 150. The points of inflexion of the erosion curves, which are of major importance for the evaluation of experimental results, were determined from third degree polynomials that were fitted to the erosion profiles. The results are shown in Figure 8 as a function of the grid size $n$. The graph indicates that for grid sizes larger than 150 the results are again no longer subject to major changes. For all further evaluations, therefore, a grid size of at least $n = 150$ was used.

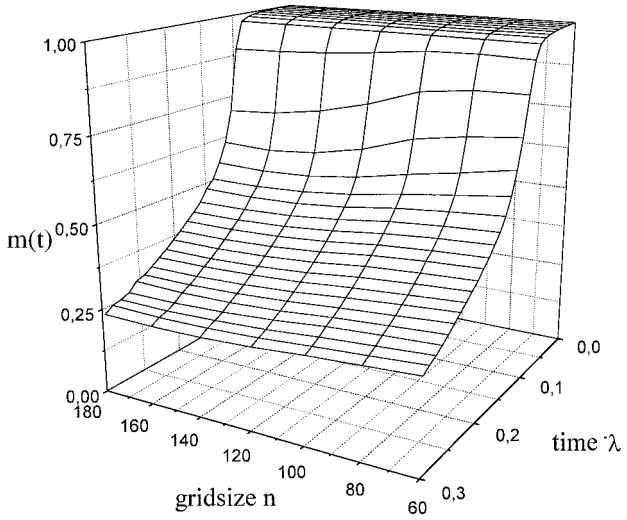


**Figure 7.** Erosion curves as a function of the gridsize $n$ (average of five simulations).

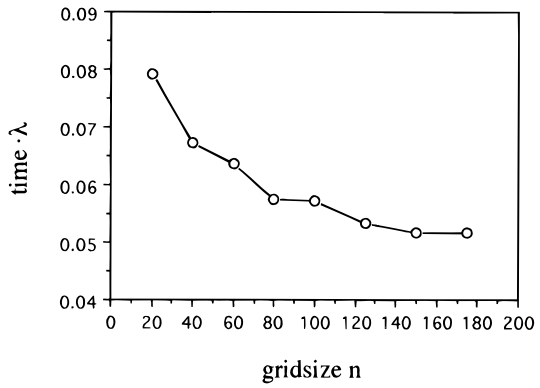


**Figure 8.** Point of inflexion in the erosion curves depending on the size of the grid (average of five simulations).

**3.4. The Evaluation of Experimental Data.** For the evaluation of experimental data, the function describing polymer erosion was fitted to experimental data by matching the points of inflexion of the theoretical and the experimental curve. To accomplish such a fit, first the point of inflexion $t_{infl}$ was determined from experimental data by fitting third degree polynomials to the curves and calculating the $x$-value by setting the second derivative equal to 0. The point of inflexion of the nondimensional erosion profile obtained for a grid of size $n = 175$ was $\lambda t = 0.052$. The degradation rate constant $\lambda_{degr}$ for experimental data can be calculated from eq 13. Once the degradation rate constant $\lambda_{degr}$ is

$$\lambda_{degr} = \frac{0.052}{t_{infl}} \tag{13}$$

known, the nondimensional $x$-axis values of the theoretical profile (Figure 5) can be transformed into time by simply dividing them by $\lambda_{degr}$. Plotting the theoretical profiles against the calculated values yields then the best fit to the experimental erosion data. Examples of profiles obtained by this fitting procedure are shown in parts a and b of Figure 9. At early times of erosion the agreement between the experimental and theoretical curves is very close. The onset of spontaneous mass loss is also described properly by the model. After this spontaneous mass loss, however, major deviations of model predictions from experimental values can be observed. The model underestimates the mass loss

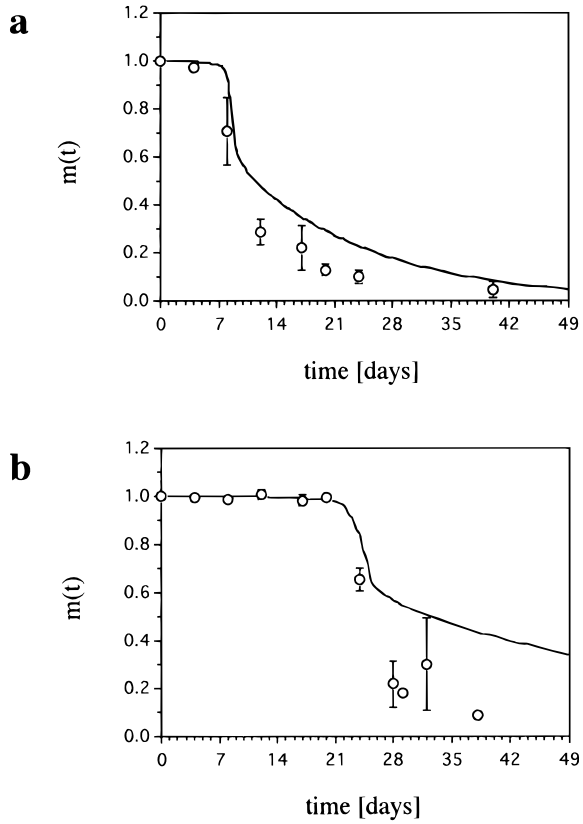


**Figure 9.** Fit of the model to experimental data of mass loss: (a) RG 502; (b) RG 502H.

**Table 1. Degradation Rate Constants Determined for Bulk-Eroding Polymers**

| polymer | $10^8\lambda_{degr}$ ($s^{-1}$) |
|---|---|
| RG 502 H | 6.9 |
| RG 502 | 2.5 |
| RG 504 H | 2.7 |

substantially. One of the reasons is the lack of the model to account for the physical erosion of the matrix during which larger pieces of the matrix may be released from the bulk without degradation. The simulation in Figure 4, for example, shows that isles of noneroded polymer on the surface are no longer connected to the matrix and could theoretically detach from the contiguous polymer. It can indeed be observed during in vitro erosion experiments that small pieces of polymer appear in the erosion medium outside the eroding matrix. Another reason that could account for the deviations of the erosion model from the experimental data may be linked to polymer swelling. Many authors have shown experimentally that a substantial water uptake of 50% and more accompanies the loss of mass.[15] At this point the physical structure of the matrix is loosened and the mass loss is accelerated, which is not taken into account by the model.

The degradation rate constants that were obtained by fitting the model to experimental data are shown in Table 1. As the hydrolysis of ordinary esters can also be described as a Poisson process the hydrolysis rate constants described in the literature have the same physical meaning as the degradation rate constants of the model. Both types of constants agree regarding the order of magnitude.[24,25] This proves that this theoretical approach is in agreement with independent data and suggests that the model rate constant is indeed related to the degradation kinetics of the polymers.

## 4. Summary and Conclusions

During polymer bulk erosion polymer degradation and polymer erosion proceed at different kinetics. While the molecular weight loss sets in right from the beginning of an experiment the mass loss profiles that represent erosion show a marked lag period. This phase of constant mass is followed by a spontaneous loss during a short period of time. The developed model is one of the first that can explain this bulk erosion phenomenon in hydrolytically degradable polymers. It explains why the mass loss profiles are sigmoid and reveals the involvement of percolation phenomena in erosion. When polymer areas within the polymer bulk degrade, they cannot erode if they have no connection to the erosion medium via pores. When the polymer is degraded to a critical degree, these degraded areas form a continuous cluster that stretches to the surface of the matrices and cause their spontaneous erosion. The only parameter that the proposed model contains is a degradation rate constant that was determined by fitting the model to experimental data obtained from the erosion of poly(D,L-lactic acid-*co*-glycolic acid) matrices. The values that were obtained in this way agree very well with the first-order hydrolysis rate constants of esters. Despite the good agreement between model and experimental data early during erosion there are deviations late during erosion, which is most likely due to the simplifications that were made for the development of the model. Processes such as the loss of small contiguous polymer pieces as well as polymer swelling that both might accelerate erosion were not taken into account. This can explain the underestimation of mass loss by the model. Such phenomena will have to be taken into account when improving the model in future studies. Despite these limitations the proposed model can help to better understand the behavior of bulk-eroding biodegradable materials and might facilitate the use of these materials in a more efficient way in future applications.

**Acknowledgment.** Special thanks are due to the Deutsche Forschungsgemeinschaft (DFG), Bonn, Germany, who sponsored this project by grant GO 565/3-1. Thanks are also due to Boehringer Ingelheim, Ingelheim, Germany, for providing the polymers.

## Abbreviations

| | |
|---|---|
| $d(t)$ | relative number of noneroded pixels at time $t$ |
| $e(t)$ | probability that a pixel degrades at time $t$ |
| $e(t)_{exp}$ | expected lifetime of a pixel (s) |
| $e(t)_{exp_n}$ | expected lifetime of $n^2$ pixels (s) |
| $e(t)_n$ | probability that a pixel located on a grid of size $n$ degrades at time $t$ |
| $\epsilon$ | random variable that is equally distributed in [0,1] |
| $\lambda$ | degradation rate constant ($s^{-1}$) |
| $\lambda_{degr}$ | degradation rate constant determined from experimental data ($s^{-1}$) |
| $m(t)$ | relative mass of noneroded polymer at time $t$ |
| $n$ | grid size |
| $P_{i,j}$ | pixel on the computational at $i, j$ |
| $t$ | time (s) |
| $t_{i,j}$ | time at which pixel $P_{i,j}$ degrades (s) |
| $t_{infl}$ | point of inflexion in an experimental mass loss profile (s) |
| $x_{i,j}$ | function defining the status of a pixel as crystalline, amorphous, or eroded |

## References and Notes


(1) Leenslang, J. W.; Pennings, A. J.; Ruud, R. M.; Rozema, F. R.; Boering, G. Resorbable materials of poly(L-lactide). VI. Plates and screws for internal fracture fixation. *Biomaterials* **1987**, *8*, 70−73.

(2) Peppas, N. A.; Langer, R. New challanges in biomaterials. *Science* **1994**, *263*, 1715−1720.

(3) Kenley, R. A.; Lee, M. O.; Mahoney, T. R., II; Sanders, L. M. Poly(lactide-*co*-glycolide) decomposition kinetics in vivo and in vitro. *Macromolecules* **1987**, *20*, 2398−2403.

(4) Tamada, J.; Langer, R. Erosion mechanism of hydrolytically degradable polymers. *Proc. Natl. Acad. Sci. U.S.A.* **1993**, *90*, 552−556.

(5) Langer, R.; Peppas, N. Chemical and physical structure of polymers as carriers for controlled release of bioactive agents: a review. *J. Macromol. Sci.—Rev. Macromol. Chem. Phys.* **1983**, *C23*, 61−126.

(6) Heller, J. Use of poly(ortho esters) and polyanhydrides in the development of peptide and protein delivery systems. In *Formulation and Delivery of Proteins and Peptides*; Cleland, J. L., Langer, R., Eds.; ACS Symposium Series 567; American Chemical Society: Washington, DC, 1994; pp 292−305.

(7) Göpferich, A.; Langer, R. Polymer erosion. *Macromolecules*, **1993**, *26*, 4105−4112.

(8) Zygourakis, K. Discrete simulations and bioerodible controlled release systems. *Polym. Prepr. (Am. Chem. Soc., Div. Polym. Chem.)* **1989**, *30*, 456−457.

(9) Zygourakis, K. Development and temporal evolution of erosion fronts in bioerodible controlled release devices. *Chem. Eng. Sci.* **1990**, *45*, 2359−2366.

(10) Asano, M.; Fukuzaki, H.; Yoshida, M.; Kumakura, M.; Mashimo, T.; Yuasa, H.; Imai, K.; Yamanaka, H.; Kawaharada, U.; Suzuki, K. In vivo controlled release of a luteinizing hormone-releasing hormone agonist from poly(D,L-lactic acid) formulations of varying degradation pattern. *Int. J. Pharm.* **1991**, *67*, 67−77.

(11) Asano, M.; Fukuzaki, H.; Yoshida, M.; Kumakura, M.; Mashimo, T.; Yuasa, H.; Imai, K.; Yamanaka, H. Application of poly(D,L-lactic acids) of varying molecular weight in drug delivery systems. *Drug Des. Delivery* **1990**, *5*, 301−320.

(12) Zhang, X.; Wyss, U. P.; Pichora, D.; Goosen, M. F. A. An investigation of poly(lactic acid) degradation. *J. Bioact. Compat. Polym.* **1994**, *9*, 80−101.

(13) Holland, S. J.; Jolly, A. M.; Yasin, M.; Tighe, B. J.; Polymers for biodegradable medical devices II. Hydroxybutyrate−hydroxyvalerate copolymers: hydrolytic degradation studies. *Biomaterials* **1987**, *8*, 289−295.

(14) Li S., M.; Garreau, H.; Vert, M. Structure−property relationships in the case of the degradation of massive aliphatic poly-(α-hydroxy acids) in aqueous media, part 1: poly(DL-lactic acid). *J. Mater. Sci. Mater. Med.* **1990**, *1*, 123−130.

(15) Li S., M.; Garreau, H.; Vert, M. Structure−property relationships in the case of the degradation of massive poly(α-hydroxy acids) in aqueous media part 2: degradation of lactide−glycolide copolymers: PLA37.5GA25 and PLA75GA25. *J. Mater. Sci. Mat. Med.* **1990**, *1*, 131−139.

(16) Li, S. M.; Garreau, H.; Vert, M. Structure−property relationships in the case of the degradation of massive poly(α-hydroxy acids) in aqueous media, Part 3: influence of the morphology of poly(L-lactic acid). *J. Mater. Sci. Mat. Med.* **1990**, *1*, 198−206.

(17) Herrlinger, M. In Vitro Polymerabbau und Wirksttofffreigabe von Poly-DL-Laktid-Formlingen, Ph.D. Thesis, Heidelberg, Germany, 1994.

(18) Mäder, K.; Stosser, R.; Borchert, H.-H.; Mank, R.; Nerlich, B. ESR-Untersuchung zur Wasserpenetration in Polymerfolien und Mikropartikeln auf der Basis von biologisch abbaubaren Polyestern. *Pharmazie* **1991**, *46*, 342−345.

(19) Göpferich, A.; Langer, R. The influence of microstructure and monomer properties on the erosion mechanism of a class of polyanhydrides. *J. Polym. Sci.* **1993**, *31*, 2445−2458.

(20) Shah, S. S.; Cha, Y.; Pitt, C. G. Poly(glycolic acid-*co*-D,L-lactic acid): diffusion or degradation controlled drug delivery. *J. Controlled Release* **1992**, *18*, 261−270.

(21) Zhu, J.-H.; Shen, Z.-R.; Wu, L.-T.; Yang, S.-L. In vitro degradation of polylactide and poly(lactide-*co*-glycolide) microspheres. *J. Appl. Polym. Sci.* **1991**, *43*, 2099−2106.

(22) Drake, A. W. *Fundamentals of applied probability theory*; McGraw-Hill: New York, 1988; pp 129−144.

(23) Kalos, M. H.; Whitlock, P. A. *Monte Carlo Methods*; Wiley: New York; 1986; p 7.

(24) Kirby, A. J. Hydrolysis and formation of esters of organic acids. In *Comprehensive Chemical Kinetics Volume 10: Ester Formation and Hydrolysis and Related Reactions*; Bamford, C. H., Tipper, C. F. H., Eds.; Elsevier: Amsterdam, 1972; pp 57−202.

(25) Park, K.; Shalaby, W. S. W.; Park H. *Biodegradable Hydrogels for Drug Delivery*; Technomic Publ.: Lancaster, PA, 1993.


MA961627Y